Asian Journal of Water, Environment and Pollution. Vol. 22, No. 5 (2025), pp. 165-178.
doi: 10.366922/AJWEP025150108

ORIGINAL RESEARCH ARTICLE

Phosphorus alleviates aluminum toxicity in *Camellia oleifera* seedlings by regulating the leaf metabolic profile: Insights from metabolomics

Yi Wang[1,2]*, Xing Chen[2], Yongquan Li[2]*, and Aiai Xu[1]

[1]Institute of Resources, Environment and Soil Fertilizer, Fujian Academy of Agricultural Sciences/Fujian Key Laboratory of Plant Nutrition and Fertilizer, Fuzhou, Fujian, China

[2]Department of Forestry, College of Horticulture and Landscape Architecture, Zhongkai University of Agriculture and Engineering, Guangzhou, Guangdong, China

***Corresponding authors:** Yi Wang (wangyi@zhku.edu.cn)
Yongquan Li (yongquanli@zhku.edu.cn)

Received: April 8, 2025; Revised: June 7, 2025; Accepted: June 11, 2025; Published online: July 22, 2025

Abstract: *Camellia oleifera* Abel, recognized as one of the world's four major woody edible oil sources, is extensively cultivated in the acidic red soil regions in southern China. This study focused on *C. oleifera* seedlings to investigate the mechanisms through which phosphorus (P) mitigates aluminum (Al) toxicity. The seedlings were subjected to various P–Al solutions at different concentration ratios, and a metabolomic analysis of their leaves was then conducted. The analysis identified a total of 509 metabolites, predominantly flavonoids and tannins. Among these, 466 flavonoids showed significant increases across all comparison groups, whereas 35 differentially abundant metabolites were consistently detected. Kyoto Encyclopedia of Genes and Genomes functional annotation and enrichment analysis highlighted the isoflavone biosynthesis pathway as the most significantly enriched pathway among the differentially abundant metabolites. Key metabolites identified as significantly differentially abundant included glycitin, naringenin, and 3,9-dihydroxypterocarpan. This research elucidates the metabolic alterations in *C. oleifera* seedlings under P and Al stress, suggesting that changes in flavonoid metabolites and the activation of the isoflavone biosynthesis pathway may be crucial adaptive strategies for *C. oleifera* to withstand such stresses. The findings not only offer a theoretical foundation for enhancing plant stress resistance but also provide valuable insights into the cultivation and management practices of *C. oleifera*.

Keywords: *Camellia oleifera*; Aluminum toxicity; Phosphorus; Flavonoids; Metabolomic

1. Introduction

In non-acidic soils, aluminum (Al) typically exists in the form of insoluble aluminosilicates and Al oxides,[1] which have minimal impact on the growth of forest plants. However, when the pH of tropical and subtropical forestry soils drops below 5.5, Al exists in the form of Al^{3+}. Excessive Al^{3+} is toxic to plants, severely restricts the growth of forest vegetation, and impacts crop yields in acidic soils.[2] Plant roots readily absorb free Al ions, and excessive accumulation of these ions typically causes manifestations of Al toxicity in plants,[3] affecting their normal development and growth.[4,5] The phenomenon of acid rain in southern China is intensifying, with its impact area gradually expanding. Concurrently, soil acidification is reaching critical levels, exacerbated by

the excessive use of acidic fertilizers and unsustainable agricultural practices.[6]

Globally, about 30% of arable land and nearly half of potentially cultivable land are experiencing significant soil acidification, as evidenced by decreasing soil pH levels, which leads to an excess of soluble Al ions in the soil.[7,8] Plants alleviate Al toxicity by releasing organic acids (such as malate and citrate) into the rhizosphere, where these acids form stable, non-toxic complexes with Al ions, thereby reducing their phytotoxic effects.[9] Due to their prolonged exposure to soil environments, plant root tissues generally demonstrate the highest sensitivity to Al stress among all plant parts. The inhibitory effect of Al on root growth in soybean plants (*Glycine max* [L.] Merr.) becomes evident within merely five minutes of exposure at a remarkably low Al concentration of 75 μmol/L.[10] Kochian *et al.*[11] reported that Al ions can combine with pectin and other components in the root cell wall, disrupting its structure, impairing its function, and subsequently inhibiting the growth of aboveground parts. Recent studies demonstrate that an *Agrobacterium tumefaciens*-loaded microneedle delivery system successfully transfers the green fluorescent protein gene into both apical meristems and leaves of tobacco (*Nicotiana tabacum*) plants, achieving stable transgene expression and enhanced stress resistance.[12] This approach provides a novel platform for the efficient delivery of stress-resistance genes in plant biotechnology. Yu *et al.*[13] demonstrated that Al stress significantly inhibits rapeseed growth, particularly through the reduction of root length and biomass. Notably, cerium oxide nanoparticles can improve the growth performance of rapeseed and cotton seedlings under salt stress by scavenging and eliminating excess reactive oxygen species (ROS), thereby enhancing their salt tolerance.[14] Similarly, in hybrid *Liriodendron chinense*, Al stress not only restricts growth but also disrupts cellular redox homeostasis, leading to the accumulation of ROS. Notably, the application of xiaminobutyric acid (GABA) has been shown to mitigate these adverse effects by enhancing plant growth parameters, such as biomass and root length. Furthermore, GABA treatment increases the activity of key antioxidant enzymes, such as peroxidase and superoxide dismutase, thereby restoring redox balance.[15] Parallel observations have been made in alfalfa, where Al stress results in a substantial accumulation of Al ions in both root and shoot tissues, subsequently elevating ROS levels and inducing oxidative stress.[16]

Phosphorus (P) is a crucial element required for the growth and development of plants. It is among the essential elements for the synthesis of phospholipids, nucleic acids, adenosine triphosphate, and other biological macromolecules and is involved in various metabolic activities of plants.[17] In acidic soils, P deficiency and Al toxicity often occur simultaneously, which restricts the growth of plants.[18] However, in acidic soils, P readily couples with excess Al ions produced by leaching, and thus, the available P content in the soil that can be used by plants is extremely low, which has a great impact on the growth and metabolism of plants.[19] The combined stress of high Al and low P contents in soil has become a key factor restricting the productivity of woody plants.[20] Specifically, due to the coupling mechanism of P and Al, P has become an important target to alleviate Al stress. Sun *et al.*[21] showed that under relatively high Al stress, P increased the Al resistance of *Lespedeza bicolor*, an Al-tolerant species, and promoted the growth of its aboveground parts. Liu *et al.*[22] studied Chinese fir seedlings and reported that the height and length of the roots of Chinese fir seedlings increased in response to the addition of exogenous P, indicating that P alleviated the growth of Chinese fir seedlings under Al stress.

Camellia oleifera Abel, a member of the Camelliaceae family, is extensively cultivated in the acidic red soil regions in southern China,[23] and is renowned for producing one of the world's four major woody edible oils. Al plays a pivotal role in the soil environment, influencing the growth of *C. oleifera*. Excessive soil leaching results in acidic soils that are rich in Al but deficient in P, which significantly hampers the development and yield of *C. oleifera*. The expansion of acid rain-affected areas in southern China, coupled with the misuse of acidic fertilizers and inappropriate tillage practices, has exacerbated the conversion of insoluble Al into its toxic forms, such as Al^{3+}, $Al(OH)^{2+}$, and $Al(OH)^{2+}$. Furthermore, the prevalent issue of extensive management in *C. oleifera* forests makes the plants particularly susceptible to the detrimental effects of excessive Al ion toxicity. Recent advancements in metabolomics have opened new avenues for investigating the mechanisms through which P mitigates Al toxicity. Under Al stress, notable changes are observed in the morphology and flavonoid content of *C. oleifera* leaves. Specifically, there is a significant increase in the total flavonoid content and enhanced antioxidant activity in leaf extracts. Flavonoids are believed to aid in Al detoxification by scavenging ROS or forming Al chelates, thereby alleviating the toxic impact of Al on *C. oleifera* and playing a crucial role in the plant's response to Al toxicity.[24] In addition, research

indicates that Al stress induces an increase in flavonoid metabolites in wheat, which primarily assist in binding Al ions and solubilizing P in the soil, thereby reducing Al uptake.[25] These findings underscore the importance of flavonoids in enhancing plant resilience to Al stress and improving P availability in acidic soils.

Metabolomics can be used to identify metabolic phenotypes, obtain qualitative and quantitative data on many metabolites, construct metabolic networks, and predict the functions of metabolites.[26] Multivariate statistical analysis and liquid chromatography-tandem mass spectrometry (LC-MS/MS) have revealed significant differences in flavonoids in *Coreopsis tinctoria* from different production areas. Different geographical conditions and altitudes may lead to different metabolic mechanisms of flavonoids in *Coreopsis tinctoria*, which in turn affect its medicinal value.[27] In this study, *C. oleifera* seedlings were utilized as experimental materials. The study entailed administering varying concentrations of P and Al to the seedlings, followed by metabolite analysis using ultrahigh-performance LC-MS/MS (UPLC-MS/MS). This approach enabled the elucidation of the metabolic regulatory network underlying the complex interaction between P and Al. Furthermore, the research focused on exploring the critical role of metabolites in the mechanism by which P mitigates Al toxicity.

2. Materials and methods

2.1. Plant material and sample collection

C. oleifera seedlings were used as experimental subjects, and healthy plants at the same growth stage were selected for experiments. The seedlings were treated with a nutrient solution containing a combination of one of two P concentrations (0 or 0.5 mM KH_2PO_4) and one of two Al concentrations (0 or 4 mM $AlCl_3{\cdot}Al_2O$) at pH 4.2. Seedlings were randomly divided into three treatment groups: A_P5 (0 mmol/L Al, 0.5 mmol/L P), A4P5 (4 mmol/L Al, 0.5 mmol/L P), and A4P_ (4 mmol/L Al, 0 mmol/L P) (Figure 1). *C. oleifera* seedlings were treated with nutrient solutions containing different combinations of P and Al concentrations. Treatments were administered to each group at three-day intervals. After 2 months of treatment, the leaves of *C. oleifera* were harvested, cleaned thoroughly using an ultrasonic cleaner, and placed in a freezer tube for snap freezing. Three biological replicates were prepared for each treatment group. Specimens of the A_P5 treatment group were labeled A_P5-1, A_P5-2, and A_P5-3; specimens of the A4P5 treatment group were labeled A4P5-1, A4P5-2, and A4P5-3; and specimens of the A4P_ treatment group were labeled A4P_-1, A4P_-2, and A4P_-3. The samples were kept at −80°C in preparation for the downstream experiments.

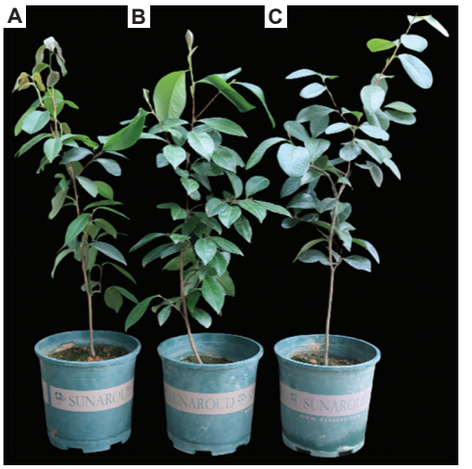

Figure 1. *Camellia oleifera* was treated with various phosphorus–aluminum solutions at different concentration ratios. (A) Group A4P_. (B) Group A4P5. (C) Group A_P5.

2.2. Pretreatment and extraction of samples

The leaf samples of *C. oleifera* were subjected to vacuum freeze-drying treatment. Subsequently, a grinderwas used to grind the samples into powder. The powdered sample was weighed (50 mg) and added to a specified internal calibration extraction solution, then vortexed once every 30 min for a total of 6 times. Once the centrifugation process was completed, the supernatant was filtered through a microporous membrane and stored in an injection bottle for UPLC-MS/MS analysis.

2.3. Instrumentation

The instruments and equipment used in this study included: a centrifuge (5424R, Eppendorf, Germany); constant-temperature metal mixer (MU-G02-0448, MIULab, China); grinder (MM 400, Retsch,Germany); one-ten-thousandth analytical balance (MS105DM, METTLER TOLEDO, Switzerland); centrifugal concentrator (CentriVap, LABCONCO, USA); lyophilizer (Scientz-100F, SCIENTZ, China); vortex mixer (VORTEX-5, Kyllin-Bell, Haimen, China); ultrasonic cleaner (KQ5200E, SUPMILE, China); pipette (Research plus, Eppendorf, Germany); automation workstation (Biomek i5, Beckman Coulter, USA); film sealing instrument (Mini HES, Monad, China).

2.4. UPLC-MS/MS conditions

A UPLC-MS/MS instrument system (ExionLC™ AD，SCIEX，USA) was employed for analysis. The same chromatographic column model as described by Wang *et al.*[24] was used. Gradient elution was performed using ultrapure water containing 0.1% formic acid (A) and acetonitrile containing 0.1% formic acid (B) as the mobile phases. The elution gradient was set according to the method described by Chu *et al.*[28] In addition, the parameters such as flow rate, column temperature, and injection volume were set with reference to studies by Wang *et al.*[27] and Chu *et al.*[28]

For mass spectrometry detection, an electrospray ionization source heated to 500°C was used. The operating parameters of this ion source were set according to the methods described by Wang *et al.*[24] and Chu *et al.*[28] Finally, quantitative analysis of the targeted metabolites was achieved by monitoring the corresponding characteristic ion pairs of the metabolites.

2.5. Qualitative and quantitative metabolite analyses

To ensure the accuracy of compound identification and the reliability of metabolite quantification, this study utilized the comprehensive compound information in the Metware database (MWDB) for compound identification. Leveraging the high sensitivity and selectivity of triple quadrupole mass spectrometry, metabolites were quantitatively analyzed using multiple reaction monitoring (MRM) mode, followed by data preprocessing. Differentially abundant metabolites were then identified through a combination of univariate and multivariate statistical analysis.

3. Results and discussion

3.1. Mass spectrometry analysis

Using the mass spectrometry data analysis software (Analyst, SCIEX, USA) along with referring to the MWDB, qualitative and quantitative analyses of the metabolites in *C. oleifera* samples are carried out. The MRM mode was employed for metabolite detection to accurately determine the compounds contained in the *C. oleifera* samples. The results are presented in a multi-peak graph in Figure 2, which intuitively shows the compounds detected in the *C. oleifera* samples. A total of 509 metabolites were detected. The main metabolites were flavonoids (91.55%) and tannins (8.45%). Among them, 466 flavonoids were identified, comprising 139 flavonols, 122 flavonoids, 54 flavanols, 40 dihydroflavones, 26 chalcones, 24 isoflavones, 21 anthocyanins, 10 dihydroflavonols, four orange ketones, and 26 unclassified flavonoids. In addition, 43 tannins were detected, including 24 gallotannins and 19 proanthocyanidins (Table S1).

3.2. Metabolite cluster analysis

Heatmaps of the metabolite content data were generated via hierarchical cluster analysis after unit variance scaling treatment (Figure 3). The results revealed differences in the accumulation patterns of metabolites across the three treatment groups. Flavonoid profiles in A4P5 differed significantly from those in A_P5 and A4P_, whereas the difference between A_P5 and A4P_ was relatively minor. Among all groups, the flavonoid content was the highest in A4P5 and the lowest in A_P5.

3.3. Principal component analysis (PCA)

PCA, a statistical technique widely adopted in metabolomics research, enables a preliminary understanding of the overall differences in metabolites and their degree of variation across samples from different groups in this study, including A4P5, A_P5, and A4P_. This is conducive to exploring potential metabolic mechanisms. As seen in Figure 4, the samples in different groups show different distributions, which indicates that

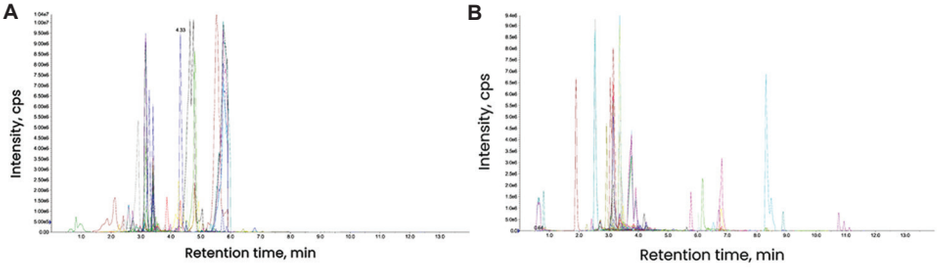

Figure 2. Multi-peak map of multiple reaction monitoring metabolite detection. Each chromatographic peak in a different color in the figure represents an individual detected metabolite. (A) Negative ion mode. (B) Positive ion mode. The x-axis shows the retention time of metabolite detection, while the y-axis displays the ion current intensity (measured in counts per second, cps).

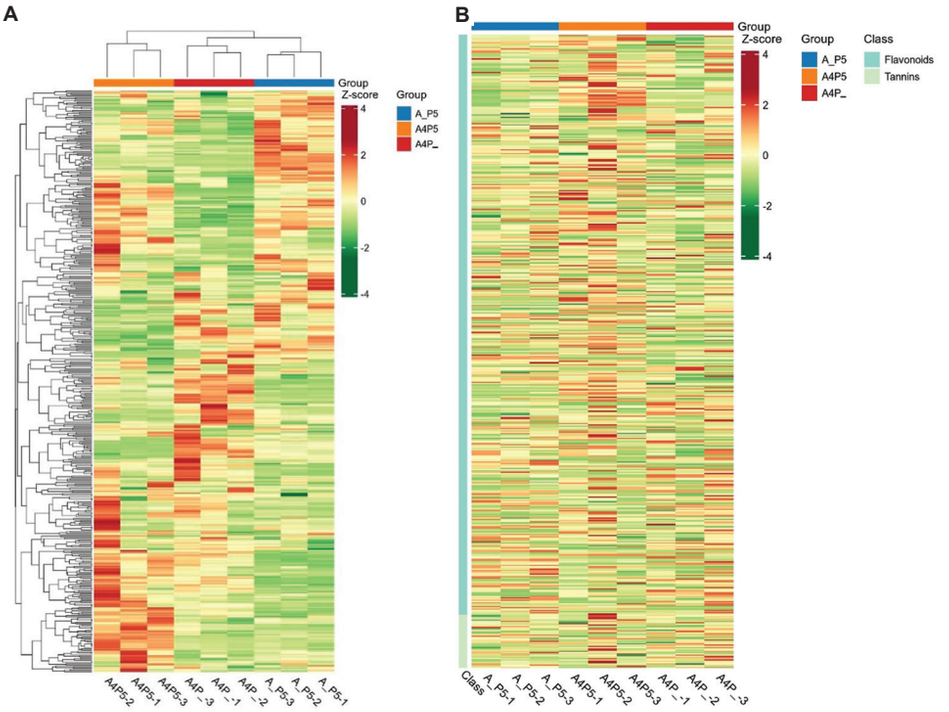

Figure 3. Hierarchical clustering diagram of 509 metabolites. The annotation bar above the heatmap corresponds to the sample grouping, while the annotation bar on the left side of the heatmap corresponds to the primary classification of compounds. Different colors represent different compound categories. In the heatmap, different colors reflect the relative content levels of metabolites: Red indicates higher content levels, while green indicates lower content levels. (A) Both metabolites and samples were subjected to cluster analysis. The clustering tree on the left side of the figure represents metabolite clustering, while the clustering tree on the top represents sample clustering. (B) Heatmap of substance classification, where "Class" denotes the primary classification of substances.

the metabolomics between the groups tends to diverge. This result suggests that the metabolite compositions of the samples differ across treatment groups. The metabolite profiles of *C. oleifera* seedlings among all treatment groups were investigated. After performing PCA on the grouped samples of A4P5, A_P5, and A4P_ for difference comparison, the principal component (PC) scores indicate that the first PC (PC1) and the second PC (PC2) play a significant role in differentiating samples. They can effectively reveal the internal differences and main changing trends across the samples. Specifically, the interpretation rates of PC1 and PC2 achieve 29.87% and 28.38%, respectively, for a total contribution rate of 70.14%. The metabolites in A4P5 significantly differed from those in A_P5 and A4P_.

3.4. Orthogonal partial least squares discriminant analysis of differentially abundant metabolites

Compared with PCA, partial least squares discriminant analysis (PLS-DA) maximizes the discrimination between groups, which is conducive to finding differentially abundant metabolites and solves the issue of insensitivity to variables with less correlation. The orthogonal partial least squares discriminant analysis (OPLS-DA), which integrates the orthogonal signal correction (OSC) and PLS-DA methods, can effectively identify and extract feature variables that are highly correlated with the response variables. At the same time, it can eliminate the variations caused by irrelevant factors, thus improving the predictive ability and interpretability of the model. The prediction parameters of the OPLS-DA evaluation model are R^2X, R^2Y, and Q^2, and a value of $Q^2 > 0.9$ is considered an excellent model. In this study, the OPLS-DA model was used to compare the samples in pairs (Figure 5): A4P5 vs. A4P_ ($R^2X = 0.651$, $R^2Y = 0.999$, $Q^2 = 0.922$, Q^2 value > 0.9); A4P5 vs. A_P5 ($R^2X = 0.674$, $R^2Y = 1$, $Q^2 = 0.946$, Q^2 value > 0.9); and A_P5 vs. A4P_ ($R^2X = 0.652$, $R^2Y = 1$, $Q^2 = 0.937$, Q^2 value > 0.9). In this study, the value

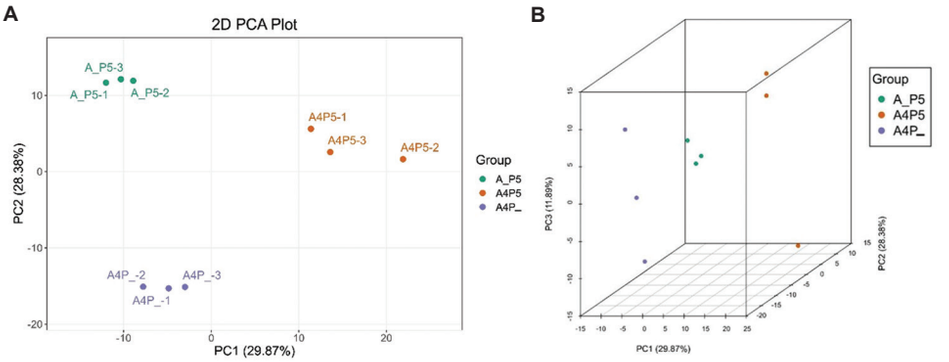

Figure 4. Differentially abundant metabolite analysis based on PCA. Each point in the graph represents a sample. Samples from the same group are represented by the same color. "Group" indicates the grouping. (A) The 2D PCA plot of differentially abundant metabolite analysis. (B) The 3D PCA plot for differentially abundant metabolite analysis. Image created by the authors.

Abbreviations: PC: Principal component; PCA: Principal component analysis.

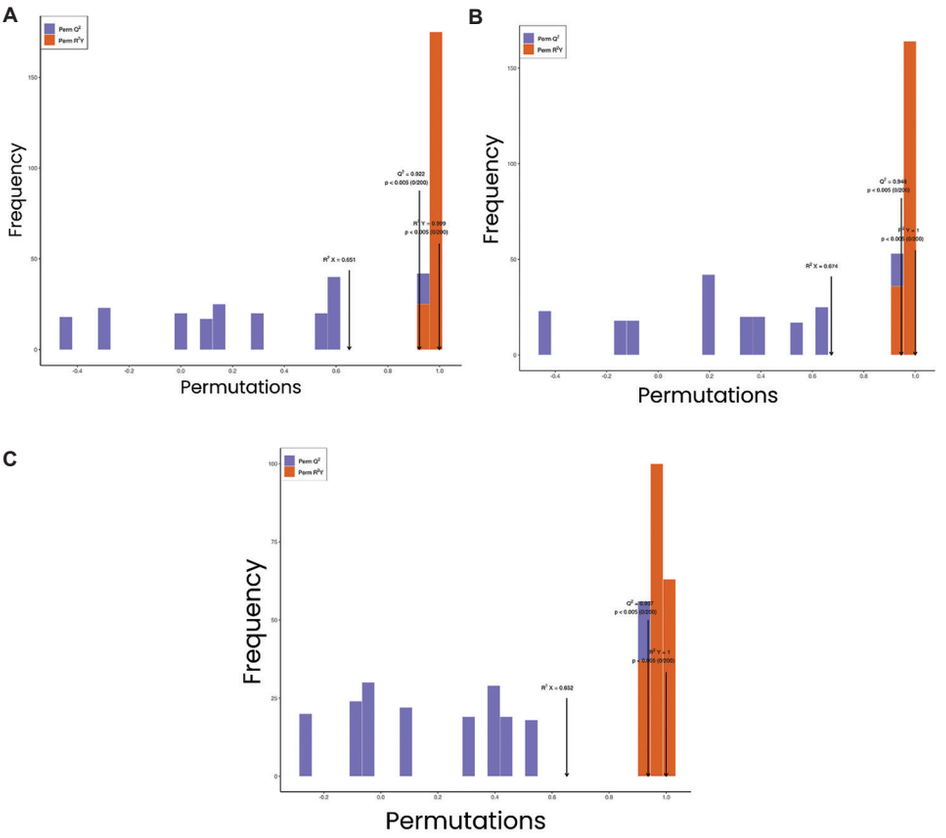

Figure 5. OPLS-DA model diagram for pairwise comparisons of differentially abundant metabolites. (A) A4P5 vs. A4P_. (B) A4P5 vs. A_P5. C) A_P5 vs. A4P_. The predictive parameters of the OPLS-DA evaluation model are R^2X, R^2Y, and Q^2. The closer these three indicators are to 1, the more stable and reliable the model is. When $Q^2 > 0.5$, the model can be considered effective; when $Q^2 > 0.9$, it is regarded as excellent.

Abbreviation: OPLS-DA: Orthogonal partial least squares discriminant analysis.

of Q^2 was close to 1, indicating the high stability and reliability of the model. This finding indicates that the model may exhibit high consistency and accuracy in prediction and analysis.

3.5. Screening of differential metabolites in *Camellia oleifera*

The screening of differential metabolites requires the combination of univariate and multivariate statistical analysis methods. Based on the results obtained from the OPLS-DA model and the fold change value, in-depth exploration from multiple angles is carried out to accurately identify differential metabolites (Table S2). Figure 6A-C shows the metabolites and differentially abundant metabolites screened in each comparison group. In different comparison groups, such as the A4P5 vs. A4P_ comparison group, the A4P5 vs. A_P5 comparison group, and the A_P5 vs. A4P_ comparison group, there were a certain number of significantly different metabolites. For the A4P5 vs. A4P_ comparison group, there were 179 significantly different metabolites, including 70 decreased metabolites and 109 increased metabolites. A total of 171 metabolites showed pronounced differences in the A4P5 vs. A_P5 comparison group, including 74 decreased metabolites and 97 increased metabolites. For the A_P5 vs. A4P_ comparison group, there were 153 metabolites with distinct differences, of which 80 were decreased metabolites and 73 were increased metabolites. Through a Venn diagram, Figure 6D illustrates the interrelationships among those metabolites that exhibit varying abundances within the three sets of comparison groups. There were 35 common differentially abundant metabolites in the A4P5 vs. A4P_ comparison group, the A4P5 vs. A_P5 comparison group, and the A_P5 vs. A4P_ comparison group, with 33, 28, and 23 unique differentially abundant metabolites, respectively.

3.6. Differentially abundant metabolite bar chart

Through qualitative and quantitative analyses of the detected metabolites, the top 20 metabolites with multiple differences in each comparison group were identified (Figure 7, Table 1). In the A4P5 vs. A4P_ comparison group, eight metabolites were increased, and 12 metabolites were decreased; in the A4P5 vs. A_P5 comparison group, 11 metabolites were increased, and nine metabolites were decreased; in the A_P5 vs. A4P_ comparison group, nine metabolites were increased, and 11 metabolites were decreased. The increased metabolites may play a key role in enhancing stress resistance.

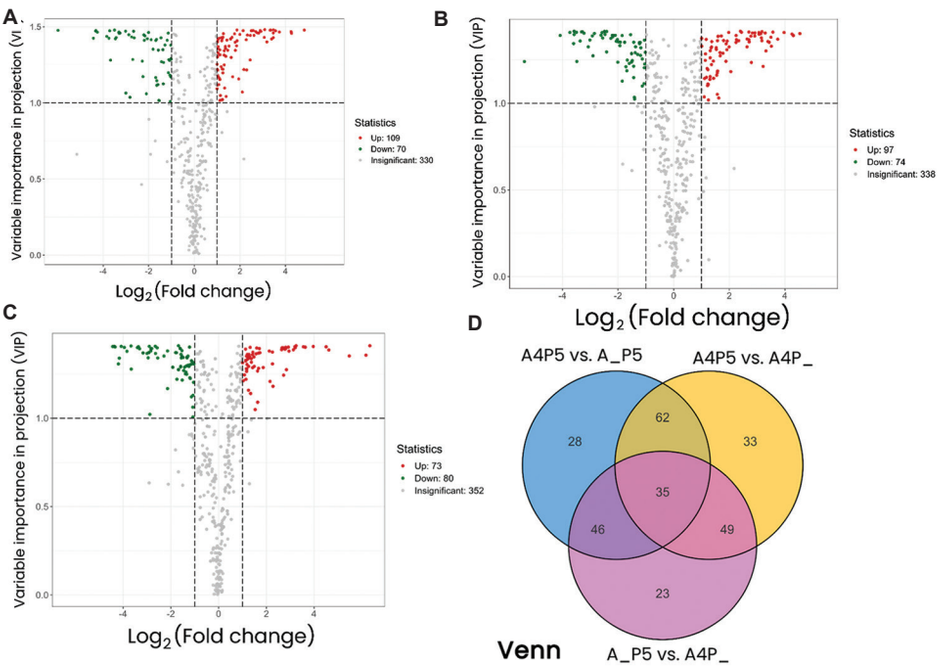

Figure 6. Volcano plot of differentially abundant metabolites. (A) A4P5 vs. A4P_. (B) A4P5 vs. A_P5. (C) A_P5 vs. A4P_. (D) Venn diagram of differentially abundant metabolites in three comparison groups. The screening criteria for differential metabolites are as follows: (i) Select metabolites with VIP > 1, as VIP > 1 is considered to have significant differences. (ii) Select metabolites with fold change ≥ 2 or fold change ≤ 0.5. Significant difference is defined by more than a 2-fold or less than 0.5-fold difference in metabolite levels between the control group and experimental groups. Image created by the authors.

Abbreviation: VIP: Variable importance in projection.

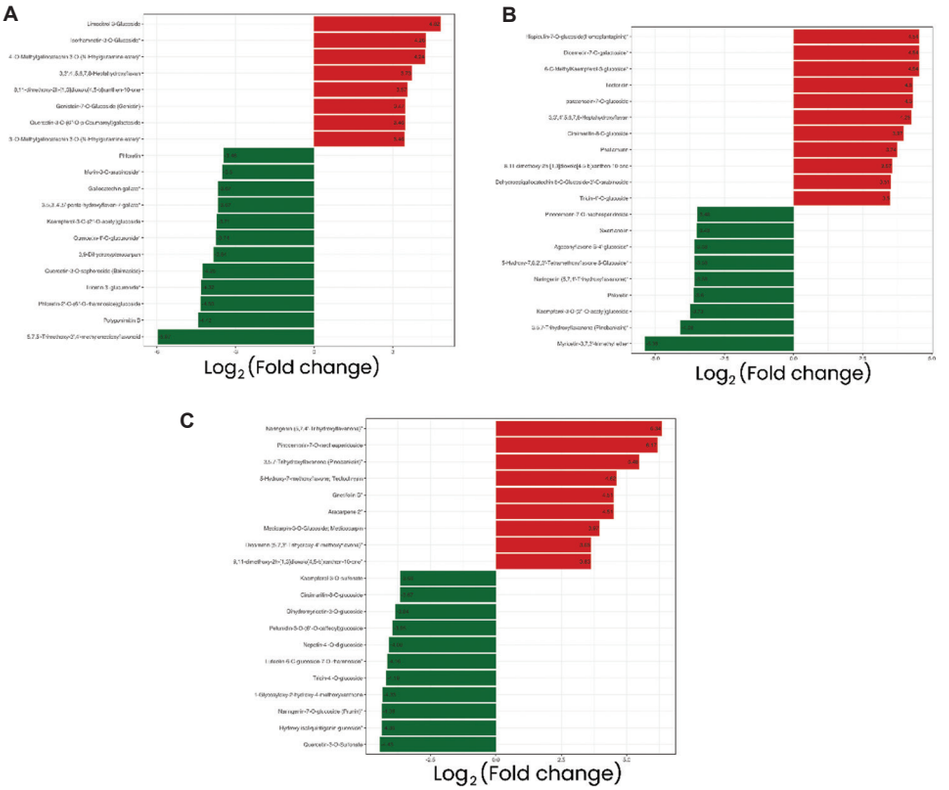

Figure 7. Bar chart of differentially abundant metabolites in three comparison groups. (A) A4P5 vs. A4P_. (B) A4P5 vs. A_P5. (C) A_P5 vs. A4P_. Red color represents an upregulation of metabolite content, while green color represents a downregulation of metabolite content. Image created by the authors.

3.7. Kyoto Encyclopedia of Genes and Genomes functional analysis of *Camellia oleifera's* differentially abundant metabolites

In this study, the Kyoto Encyclopedia of Genes and Genomes (KEGG) database was utilized to annotate the metabolites involved in this study. Figure 8 presents the annotation results of significantly different metabolites under the KEGG database. KEGG pathway enrichment analysis was then carried out based on the obtained data of differential metabolites. Considering that the nearer the *p*-value approaches zero, the greater the significance of the pathway's enrichment level, the annotation situations of these significantly different metabolites in the KEGG database were statistically screened out. The differentially abundant metabolites in the A4P5 vs. A4P_ comparison group included 173 flavonoids (66 decreased and 107 increased) and six tannins (four decreased and two increased). There were 57 metabolites in six pathways annotated by KEGG analysis, of which 18 were significantly different in their abundance. Among the six pathways with varying abundances of metabolites, the isoflavone biosynthesis pathway was significantly upregulated. In this particular pathway, the metabolites that exhibited significantly differential abundances and were annotated were glycitin, medicarpin-3-O-glucoside, naringenin, 3,9-dihydroxypterocarpan, and genistein-7-O-glucoside (genistin).

The differentially abundant metabolites in the A4P5 vs. A_P5 comparison group included 166 flavonoids (69 decreased and 97 increased) and five tannins (all decreased). There were 57 metabolites in six pathways annotated by KEGG analysis, of which the expressivity of 18 metabolites was significantly different. Among the six pathways with differentially abundant metabolites, the isoflavone biosynthesis pathway was significantly upregulated. In this pathway, the metabolites with remarkably differential abundances were daidzein-7-O-glucoside, glycitin, naringenin, and 3,9-dihydroxypterocarpan.

The differentially abundant metabolites in the A_P5 vs. A4P_ comparison groups included 147 flavonoids (78 decreased and 69 increased) and six tannins (two decreased and four increased). There were 57 metabolites in five pathways annotated by KEGG analysis, 13 of which were significantly different in

Table 1. The 36 key differentially abundant metabolites in A4P5 vs. A_P5 and A4P5 vs. A4P_

Index	Compound	Formula	Fold change	
			A4P5 vs. A_P5	A4P5 vs. A4P_
MWSslk237	Hispidulin-7-O-glucoside*	$C_{22}H_{22}O_{11}$	23.22	-
pmp000579	Diosmetin-7-O-galactoside*	$C_{22}H_{22}O_{11}$	23.22	-
Lmjp003655	6-C-Methylkaempferol-3-glucoside*	$C_{22}H_{22}O_{11}$	23.22	-
MWSslk013	Tectoridin	$C_{22}H_{22}O_{11}$	19.73	-
Zmgp004060	paratensein-7-O-glucoside	$C_{22}H_{22}O_{11}$	19.73	-
Lajp002709	3,3’,4’,5,6,7,8-Heptahydroxyflavan	$C_{15}H_{14}O_{8}$	19.09	13.27
Lmnp003184	Cirsimaritin-8-C-glucoside	$C_{23}H_{24}O_{11}$	15.68	-
pmp000531	Phellamurin	$C_{26}H_{30}O_{11}$	13.35	-
Wbtp004798	8,11-dimethoxy-2h-(1,3) dioxolo (4,5-b) xanthen-10-one	$C_{16}H_{12}O_{6}$	11.84	11.84
Wacyn03685	Dehydroepigallocatechin 6-C-glucoside-3’-C-arabinoside	$C_{26}H_{30}O_{15}$	11.40	-
Lmhp206353	Tricin-4’-O-glucoside	$C_{23}H_{24}O_{12}$	11.29	-
HJN076	Pinocembrin-7-O-neohesperidoside	$C_{27}H_{32}O_{13}$	0.09	-
Wbtp004648	Swertianolin	$C_{20}H_{20}O_{11}$	0.09	-
Layp005773	Ageconyflavone B-4’-glucoside*	$C_{25}H_{28}O_{12}$	0.08	-
Wagp005813	5-Hydroxy-7,8,2’,3’-tetramethoxyflavone 5-glucoside*	$C_{25}H_{28}O_{12}$	0.08	-
pme0376	Naringenin*	$C_{15}H_{12}O_{5}$	0.08	-
pme1201	Phloretin	$C_{15}H_{14}O_{5}$	0.08	0.09
ZBN0303	Kaempferol-3-O-(2’’-O-acetyl) glucoside	$C_{23}H_{22}O_{12}$	0.08	0.08
mws0914	3,5,7-Trihydroxyflavanone*	$C_{15}H_{12}O_{5}$	0.06	-
Lmfn004235	Myricetin-3,7,3’-trimethyl ether	$C_{18}H_{16}O_{8}$	0.02	-
Wagp004984	Limocitrol 3-glucoside	$C_{24}H_{26}O_{14}$	-	28.29
Zbpp001992	Isorhamnetin-3-O-glucoside*	$C_{22}H_{22}O_{12}$	-	19.19
CYp003396	4’-O-Methylgallocatechin 3-O-(N-ethylglutamine ester)*	$C_{23}H_{28}N_{2}O_{9}$	-	18.94
mws0895	Genistein-7-O-glucoside	$C_{21}H_{20}O_{10}$	-	11.06
Lmyp004052	Quercetin-3-O-(6’’-O-p-coumaroyl) galactoside	$C_{30}H_{26}O_{14}$	-	11.04
CYp003564	3’-O-Methylgallocatechin 3-O-(N-ethylglutamine ester)*	$C_{23}H_{28}N_{2}O_{9}$	-	11.02
Lmfn004065	Morin-3-O-arabinoside*	$C_{20}H_{18}O_{11}$	-	0.09
MWSN0066	Gallocatechin gallate*	$C_{22}H_{18}O_{11}$	-	0.08
ZBN0396	3,5,3’,4’,5’-penta-hydroxyflavan-7-gallate*	$C_{22}H_{18}O_{11}$	-	0.08
Lmfn003760	Quercetin-4’-O-glucuronide*	$C_{21}H_{18}O_{13}$	-	0.07
Lmdn007639	3,9-Dihydroxypterocarpan	$C_{15}H_{12}O_{4}$	-	0.07
MWSHY0162	Quercetin-3-O-sophoroside	$C_{27}H_{30}O_{17}$	-	0.05
Wayn004603	Tricetin 3’-glucuronide*	$C_{21}H_{18}O_{13}$	-	0.05
Zbpn004570	Phloretin-2’-O-(6’’-O-rhamnoside) glucoside	$C_{27}H_{34}O_{14}$	-	0.05
Zmhn001934	Polygonimitin B	$C_{21}H_{22}O_{9}$	-	0.05
Hagn002504	5,7,5’-Trimethoxy-3’,4’-methylenedioxyflavonoid	$C_{19}H_{16}O_{7}$	-	0.02

Note: - indicates no significant differential changes were detected; * indicates isomer.

abundance. Among the five pathways with differentially abundant metabolites, the isoflavone biosynthesis pathway was upregulated significantly. The metabolites annotated in this pathway and had pronouncedly differential abundances were glycitin, medicarpin-3-O-glucoside, naringenin, and genistin.

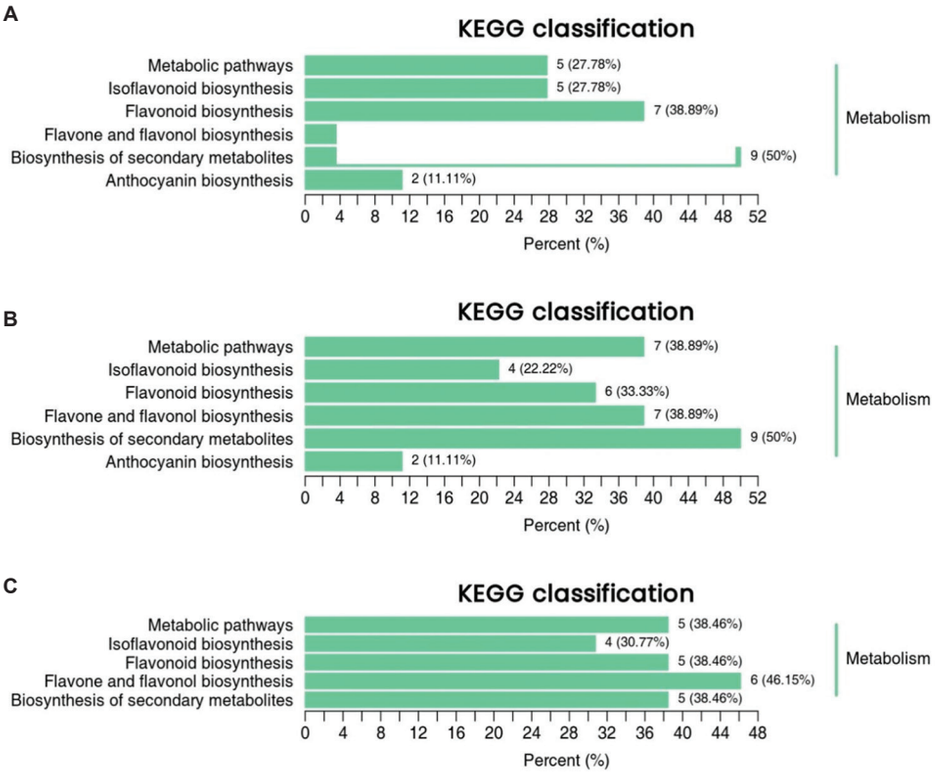

Figure 8. Pathway classification diagram of differentially abundant metabolites. (A) A4P5 vs. A4P_. (B) A4P5 vs. A_P5. (C) A_P5 vs. A4P_. The y-axis represents the names of metabolic pathways, with the x-axis representing the number of differential metabolites annotated to each pathway and the proportion of this number to the total number of annotated differential metabolites. Image created by the authors.
Abbreviation: KEGG: Kyoto Encyclopedia of Genes and Genomes.

4. Discussion

The environment plays a vital role in influencing the biosynthesis of plant secondary metabolites, ranking among the most significant factors. Al, being the principal constituent of soil minerals, can be found in a diversity of primary minerals.[29] When the soil pH is less than 5.5, the Al in the soil begins to dissolve, and plant roots can conveniently assimilate the solubilized Al in the form of Al^{3+}, even in trace quantities (micromolar concentrations of Al). In such cases, plant growth will be inhibited, and the absorption of nutrients and water will be attenuated, resulting in a decrease in fruit yield.[30] Among the secondary metabolites in plants, flavonoids represent a crucial category[31] and play vital roles in plant growth and plant-environment interactions.[32] As an essential component of the plant defense mechanism, flavonoids exert significant influences in helping plants cope with individual stressors, such as metal ions or salt, as well as combined stressors, such as temperature fluctuations and drought conditions.[33]

In this study, the metabolites of different treatment groups were identified and analyzed using a UPLC-MS/MS detection platform. In total, 509 metabolites were identified, demonstrating that plant metabolite profiles change under specific conditions and providing an important basis to further understand the response mechanism of *C. oleifera* seedlings under P and Al stress. The overall analysis of metabolites revealed that flavonoids and tannins were the main metabolite categories, of which flavonoids accounted for 91.55%. Flavonoids have many important physiological functions in plants. Studies have shown that flavonoids in plant roots respond to Al stress by binding to Al entering the cells. This interaction results in reduced potassium uptake, which plays a role in scavenging ROS generated by Al and P stress.[34] In addition, flavonoids play a crucial role in plant ontogeny, and their levels are positively correlated with plant growth and development.[35] Flavonoids have antioxidant effects, scavenging free radicals and protecting plant cells from oxidative damage.[36]

In addition, flavonoids fulfill crucial functions, such as enhancing plant resistance and adaptability in response to environmental pressures,[37] and play a vital role in plant defense mechanisms. Flavonoids can be used as natural antifungal agents or plant antitoxins, helping plants resist external damage.[38] In addition, the accumulation of flavonoids in plant roots can modify root structure, potentially helping to dissolve insoluble P in the soil to increase its availability.[39] In this study, the changes in flavonoid metabolites across different treatment groups may serve as important indicators of *C. oleifera* seedlings' response to P and Al stress.

The screening results for the differentially abundant metabolites revealed that many metabolites were significantly different in the comparison groups. For example, 179 metabolites exhibited substantial disparities when comparing A4P5 and A4P_ treatment groups, and in the comparison between the A4P5 and A_P5 treatment groups, 171 metabolites manifested notable discrepancies. In addition, 153 metabolites showed pronounced differences between the A_P5 and A4P_ treatment groups. In the A4P5 vs. A_P5 comparison group, under the same P conditions, 40 differentially abundant metabolites were detected in high levels after Al treatment; in the absence of Al treatment, only nine differentially abundant metabolites were detected in high levels. Among the metabolites showing differences in abundance, myricetin-3,7,3'-trimethyl ether was the most abundant differentially abundant metabolite in the absence of Al. After Al treatment, there were 13 differentially abundant metabolites detected, including petunidin-3-O-(6''-O-p-coumaroyl)rutinoside, homoeriodictyol 7-O-glucoside, tamarixetin-3-O-(6''-malonyl)glucoside, gambiriin B1, luteolin-6-C-glucoside-7-O-rhamnoside, pellamurin, hesperetin-5-O-glucoside, quercetin-4'-O-glucoside, quercetin-7-O-glucoside, kaempferol-3-O-sulfonate, quercetin-3-O-(4''-O-glucosyl)rhamnoside, 1,8-dihydroxy-4,5-dimethoxy-3-([{2s,3r,4s,5s,6r}-3,4,5-trihydroxy-6-{hydroxymethyl}oxan-2-yl]oxy)xanthen-9-one, and dehydroepigallocatechin 6-C-Glucoside-3'-C-arabinoside. In the A4P5 vs. A_P5 comparison groups, under the same P conditions, the number of differentially abundant metabolites increased from 9 to 40 after Al treatment. These differentially abundant metabolites may be involved in the process of Al detoxification. Previous studies have shown that quercetin is secreted from the roots of plants under Al stress and forms a stable, non-toxic complex by binding to Al ions, thereby reducing the toxicity of Al to plants.[40] This complex plays a key role in Al stress and has important value in the mechanism of stress resistance.

In the A4P5 vs. A4P_ comparison groups, under the same Al stress conditions, 19 differentially abundant metabolites were detected in high levels without P treatment; after P treatment, 35 differentially abundant metabolites were detected in high levels. Among the differentially abundant metabolites, in the absence of P, the metabolites with the highest levels were clitorin, kaempferol-3-O-rutinoside-7-O-rhamnoside, and quercetin-3-O-arabinoside. After P treatment, the eight differentially abundant metabolites with the highest levels were violanthin, tararixetin-3-O-(6''-malonyl)glucoside, kaempferol-3-O-neohesperidoside-7-O-glucoside, kaempferol-3-O-rutinoside-7-O-glucoside, luteolin-7-O-neohesperidoside, luteolin-7-O-rutinoside, biondnoid I, and quercetin-3-O-(4''-O-glucosyl)rhamnoside. In the A4P5 vs. A4P_ comparison group, under the same Al stress conditions, the addition of P increased the number of differentially abundant metabolites from 19 to 35. These increased metabolites may play a role in antioxidation, thereby reducing oxidative damage caused by Al stress and helping plants adapt to it.

Moreover, across the three comparison groups, 35 metabolites of common differential abundance status were detected, and each comparison group harbored its own distinctive metabolite profiles. Some researchers have studied the effects of long-term interactions of Al and P on the concentration and release of malate and citrate in citrus roots, and the results show that malate and citrate are mainly released from the root surface.[41] In the current study, the content of flavonoid metabolites in *C. oleifera* increased under P and Al stress, which may represent a coordinated response to the interaction between P and Al. In addition, plants can regulate root morphology by removing P from phosphorylated metabolites, thereby promoting the accumulation of flavonoids to address P deficiency.[42] The existence of these differentially abundant metabolites reflects the metabolic adjustment of plants under different stress conditions. The analysis of commonly differentially abundant metabolites (such as mangiferin, diosmetin, and gnetifolin B) and unique differentially abundant metabolites provides evidence for the specific responses of plants to distinct stress conditions. For example, commonly differentially abundant metabolites may be associated with the underlying defense mechanisms of plants.[43]

The KEGG functional annotation and enrichment analysis of differentially abundant metabolites showed that the isoflavone biosynthesis pathway was significantly enriched. This result is consistent with previous research indicating that isoflavones are crucial in enhancing plants' stress tolerance.[44] A higher

isoflavone content and faster isoflavone biosynthesis can provide a stronger biochemical defense basis for soybean seeds; the biosynthesis of isoflavones, especially the more active aglycones, is significantly increased in resistant genotypes, which helps to improve the resistance of soybean to field mildew stress.[45] Furthermore, numerous investigations have demonstrated that the biosynthesis of isoflavones serves as a crucial factor in the plant's stress-responsive mechanisms.[46] Moreover, isoflavones may also play a role in the stimulating effect because lower concentrations of toxic metals are beneficial to plant growth.[47] The activation of the isoflavone biosynthesis pathway may be an important strategy for plants to cope with P and Al stress. The results of our study provide an important reference for future studies on the response mechanisms of plants to P and Al stress. Under acidic soil conditions, lime application can be employed to raise the soil pH and reduce the bioavailability of active Al^{3+}. In red soil regions with severe Al toxicity, the P-Al ratio optimization strategy from this study can be adopted to guide P fertilizer application, prioritizing fast-acting P fertilizers like potassium dihydrogen phosphate to immobilize active Al.[48] This approach should be combined with organic fertilizer to enhance plant Al tolerance.

5. Conclusion

The metabolites in *C. oleifera* seedlings treated with different concentrations of P and Al in a nutrient mixture were analyzed in depth. A total of 509 metabolites were detected, among which flavonoids were the predominant metabolites, and many flavonoids showed a significant increasing trend. In the process of KEGG functional annotation and comprehensive enrichment analysis, it became evident that the isoflavone biosynthesis pathway showed substantial enrichment of differentially abundant metabolites. Glycitin, naringenin, and 3,9-dihydroxypterocarpan were significantly different metabolites. This study explored the physiological mechanism by which P availability alleviates Al toxicity in *C. oleifera* and provided valuable insights into the metabolic response of *C. oleifera* under P and Al stress. The results provide a theoretical basis for improving plant stress resistance and an important reference for the cultivation and management of *C. oleifera.*

Acknowledgments

The authors are grateful to all members of the laboratory for their technical assistance and stimulating discussions.

Funding

This research was supported by Fujian Key Laboratory of Plant Nutrition and Fertilizer, grant number 2023PNFKL21.

Conflict of interest

The authors declare they have no competing interests.

Author contributions

Conceptualization: Yi Wang, Aiai Xu
Formal analysis: Yi Wang
Investigation: Xing Chen, Yongquan Li
Methodology: Xing Chen, Yongquan Li, Aiai Xu
Writing–original draft: Yi Wang, Xing Chen
Writing–review & editing: Yi Wang, Aiai Xu

Availability of data

Not applicable.

References

1. Delhaize E, Ryan PR. Aluminum toxicity and tolerance in plants. *Plant Physiol*. 1995;107(2):315. doi: 10.1104/pp.107.2.315
2. Liu H, Zhu R, Shu K, Lv W, Wang S, Wang C. Aluminum stress signaling, response, and adaptive mechanisms in plants. *Plant Signal Behav*. 2022;17(1):2057060. doi: 10.1080/15592324.2022.2057060
3. Zhang X, Long Y, Huang J, Xia J. Molecular mechanisms for coping with Al toxicity in plants. *Int J Mol Sci*. 2019;20(7):1551. doi: 10.3390/ijms20071551
4. Kouki R, Ayachi R, Ferreira R, Sleimi N. Behavior of *Cucumis sativus* L. in presence of aluminum stress: Germination, plant growth, and antioxidant enzymes. *Food Sci Nutr*. 2021;9(6):3280-3288. doi: 10.1002/fsn3.2294
5. Ma L, Yang S. Growth and physiological response of *Kandelia obovata* and *Bruguiera sexangula* seedlings to aluminum stress. *Environ Sci Pollut Res*. 2022;29(28):43251-43266. doi: 10.1007/s11356-021-17926-0
6. Raza S, Zamanian K, Ullah S, Kuzyakov Y, Virto I, Zhou J. Inorganic carbon losses by soil acidification jeopardize global efforts on carbon sequestration and climate change mitigation. *J Clean Prod*. 2021;315:128036. doi: 10.1016/j.jclepro.2021.128036
7. von Uexküll HR, Mutert E. Global extent, development and economic impact of acid soils. *Plant Soil*.

1995;171(1):1-15.
doi: 10.1007/BF00009558

8. Chauhan DK, Yadav V, Vaculík M, *et al*. Aluminum toxicity and aluminum stress-induced physiological tolerance responses in higher plants. *Crit Rev Biotechnol*. 2021;41(5):715-730.
doi: 10.1080/07388551.2021.1874282
9. Hajiboland R, Panda CK, Lastochkina O, Gavassi MA, Habermann G, Pereira JF. Aluminum toxicity in plants: Present and future. *J Plant Growth Regul*. 2023;42(7):3967-3999.
doi: 10.1007/s00344-022-10866-0
10. Kopittke PM, Moore KL, Lombi E, *et al*. Identification of the primary lesion of toxic aluminum in plant roots. *Plant Physiol*. 2015;167(4):1402-1411.
doi: 10.1104/pp.114.253229
11. Kochian LV, Hoekenga OA, Piñeros MA. How do crop plants tolerate acid soils? mechanisms of aluminum tolerance and phosphorous efficiency. *Annu Rev Plant Biol*. 2004;55:459-493.
doi: 10.1146/annurev.arplant.55.031903.141655
12. Cao Y, Lim E, Xu M, Weng J, Marelli B. Precision delivery of multiscale payloads to tissue-specific targets in plants. *Adv Sci*. 2020;7(13):1903551.
doi: 10.1002/advs.201903551
13. Yu Y, Dong J, Li R, *et al*. Sodium hydrosulfide alleviates aluminum toxicity in *Brassica napus* through maintaining H_2S, ROS homeostasis and enhancing aluminum exclusion. *Sci Total Environ*. 2023;858:160073.
doi: 10.1016/j.scitotenv.2022.160073
14. Khan MN, Li Y, Mu Y, *et al*. Recent advances in nano-enabled plant salt tolerance: Methods of application, risk assessment, opportunities and future prospects. *J Integr Agric*. 2025;24(5):1611-1630.
doi: 10.1016/j.jia.2024.05.028
15. Wang P, Dong Y, Zhu L, *et al*. The role of γ-aminobutyric acid in aluminum stress tolerance in a woody plant, *Liriodendron chinense* × tulipifera. *Hortic Res*. 2021;8:80.
doi: 10.1038/s41438-021-00517-y
16. Liu C, Cheng H, Wang S, Yu D, Wei Y. Physiological and transcriptomic analysis reveals that melatonin alleviates aluminum toxicity in alfalfa (*Medicago sativa* L.). *Int J Mol Sci*. 2023;24(24):17221.
doi: 10.3390/ijms242417221
17. Dissanayaka DMSB, Ghahremani M, Siebers M, Wasaki J, Plaxton WC. Recent insights into the metabolic adaptations of phosphorus-deprived plants. *J Exp Bot*. 2021;72(2):199-223.
doi: 10.1093/jxb/eraa482
18. Qu X, Zhou J, Masabni J, Yuan J. Phosphorus relieves aluminum toxicity in oil tea seedlings by regulating the metabolic profiling in the roots. *Plant Physiol Biochem*. 2020;152:12-22.
doi: 10.1016/j.plaphy.2020.04.030
19. Mwende Muindi E. Understanding soil phosphorus. *Int J Plant Soil Sci*. 2019;31(2):1-18.
doi: 10.9734/ijpss/2019/v31i230208
20. Ofoe R, Thomas RH, Asiedu SK, Wang-Pruski G, Fofana B, Abbey L. Aluminum in plant: Benefits, toxicity and tolerance mechanisms. *Front Plant Sci*. 2023;13:1085998.
doi: 10.3389/fpls.2022.1085998
21. Sun QB, Shen RF, Zhao XQ, Chen RF, Dong XY. Phosphorus enhances Al resistance in Al-resistant *Lespedeza bicolor* but not in Al-sensitive *L. cuneata* under relatively high Al stress. *Ann Bot*. 2008;102(5):795-804.
doi: 10.1093/aob/mcn166
22. Liu B, Luo C, Li X, *et al*. Research on the threshold of aluminum toxicity and the alleviation effects of exogenous calcium, phosphorus, and nitrogen on the growth of Chinese fir seedlings under aluminum stress. *Commun Soil Sci Plant Anal*. 2014;45(1):126-139.
doi: 10.1080/00103624.2013.841917
23. He G, Zhang J, Hu X, Wu J. Effect of aluminum toxicity and phosphorus deficiency on the growth and photosynthesis of oil tea (*Camellia oleifera* Abel.) seedlings in acidic red soils. *Acta Physiol Plant*. 2011;33:1285-1292.
doi: 10.1007/s11738-010-0659-7
24. Wang Y, Cheng J, Wei S, *et al*. Metabolomic study of flavonoids in *Camellia drupifera* under aluminum stress by UPLC-MS/MS. *Plants*. 2023;12(7):1432.
doi: 10.3390/plants12071432
25. Luo D, Li Q, Pang F, *et al.* Commonalities and specificities in wheat (*Triticum aestivum* L.) responses to aluminum toxicity and low phosphorus revealed by transcriptomics and targeted metabolomics. *Int J Mol Sci*. 2024;25(17):9273.
doi: 10.3390/ijms25179273
26. Xia Y, Yu J, Miao W, Shuang Q. A UPLC-Q-TOF-MS-based metabolomics approach for the evaluation of fermented mare's milk to koumiss. *Food Chem*. 2020;320:126619.
doi: 10.1016/j.foodchem.2020.126619
27. Wang Y, Cheng J, Jiang W, Chen S. Metabolomics study of flavonoids in *Coreopsis tinctoria* of different origins by UPLC–MS/MS. *PeerJ*. 2022;10:e14580.
doi: 10.7717/peerj.14580
28. Chu Z, Xiong R, Peng X, Cui G, Dong L, Li W. Delineating molecular regulatory of flavonoids indicated by transcriptomic and metabolomics analysis during flower development in *Chrysanthemum morifolium* "Boju." *Int J Mol Sci*. 2024;25(19):10261.
doi: 10.3390/ijms251910261
29. Jackson ML. Aluminum bonding in soils: A unifying principle in soil science. *Soil Sci Soc Amer J*. 1963;27(1):1-10.
doi: 10.2136/sssaj1963.03615995002700010008x
30. Asmar J Jr., Santos FCVD, Dores ALDM, Barbalho MGDS. Chemical attributes as indicators of soil quality when applied to the cerrado biome:

A literature review. In: *Águas e Florestas: Desafios Para Conservação e Utilização*. 1st ed. Brasil: Editora Científica Digital; 2021. p. 131-148.
doi: 10.37885/210404155

31. Mierziak J, Kostyn K, Kulma A. Flavonoids as important molecules of plant interactions with the environment. *Molecules*. 2014;19(10):16240-16265.
doi: 10.3390/molecules191016240
32. Samanta A, Das G, Das S. Roles of flavonoids in plants. *Int J Pharm Sci Technol*. 2011;6:12-35.
33. Baskar V, Venkatesh R, Ramalingam S. Flavonoids (antioxidants systems) in higher plants and their response to stresses. In: Gupta DK, Palma JM, Corpas FJ, editors. *Antioxidants and Antioxidant Enzymes in Higher Plants*. Berlin: Springer International Publishing; 2018. p. 253-268.
doi: 10.1007/978-3-319-75088-0_12
34. Luo D, Li Q, Pang F, *et al*. Exploration of the commonalities and specificities in wheat respond to aluminum toxicity and low phosphorus via transcriptomics and targeted metabolomics study. *Int J Mol Sci.* 2024;25:9273.
doi: 10.20944/preprints202408.0689.v1
35. Ma D, Guo Y, Ali I, Lin J, Xu Y, Yang M. Accumulation characteristics of plant flavonoids and effects of cultivation measures on their biosynthesis: A review. *Plant Physiol Biochem*. 2024;215:108960.
doi: 10.1016/j.plaphy.2024.108960
36. Shen N, Wang T, Gan Q, Liu S, Wang L, Jin B. Plant flavonoids: Classification, distribution, biosynthesis, and antioxidant activity. *Food Chem*. 2022;383:132531.
doi: 10.1016/j.foodchem.2022.132531
37. Shomali A, Das S, Arif N, *et al*. Diverse physiological roles of flavonoids in plant environmental stress responses and tolerance. *Plants* (*Basel*). 2022;11(22):3158.
doi: 10.3390/plants11223158
38. Harborne JB, Williams CA. Advances in flavonoid research since 1992. *Phytochemistry*. 2000;55(6):481-504.
doi: 10.1016/S0031-9422(00)00235-1
39. Zhou Y, Olt P, Neuhäuser B, *et al*. Loss of LaMATE impairs isoflavonoid release from cluster roots of phosphorus-deficient white lupin. *Physiol Plant*. 2021;173(3):1207-1220.
doi: 10.1111/ppl.13515
40. Chandra J, Keshavkant S. Mechanisms underlying the phytotoxicity and genotoxicity of aluminum and their alleviation strategies: A review. *Chemosphere*. 2021;278:130384.
doi: 10.1016/j.chemosphere.2021.130384
41. Lin ZH, Chen LS, Chen RB, *et al*. Root release and metabolism of organic acids in tea plants in response to phosphorus supply. *J Plant Physiol*. 2011;168(7):644-652.
doi: 10.1016/j.jplph.2010.09.017
42. Luo J, Liu Y, Zhang H, *et al*. Metabolic alterations provide insights into Stylosanthes roots responding to phosphorus deficiency. *BMC Plant Biol*. 2020;20(1):85.
doi: 10.1186/s12870-020-2283-z
43. Saddique M, Kamran M, Shahbaz M. Differential responses of plants to biotic stress and the role of metabolites. In: Ahmad P, Ahanger MA, Singh VP, Tripathi DK, Alam P, Alyemeni MN, editors. *Plant Metabolites and Regulation Under Environmental Stress*. Ch. 4. United States: Academic Press; 2018. p. 69-87.
doi: 10.1016/B978-0-12-812689-9.00004-2
44. Lephatsi M, Nephali L, Meyer V, *et al.* Molecular mechanisms associated with microbial biostimulant-mediated growth enhancement, priming and drought stress tolerance in maize plants. *Sci Rep.* 2022;12(1):10450.
doi: 10.1038/s41598-022-14570-7
45. Deng J, Qin W, Yang C, *et al*. Seed quality deterioration dynamics for isoflavones biosynthesis in soybean (*Glycine max* L. Merr.) seeds against field mildew stress. *Acta Physiol Plant*. 2019;41(5):57.
doi: 10.1007/s11738-019-2845-6
46. Trush K, Pal'ove-Balang P. Biosynthesis and role of isoflavonoids in legumes under different environmental conditions. *Plant Stress*. 2023;8:100153.
doi: 10.1016/j.stress.2023.100153
47. Woźniak A, Drzewiecka K, Kęsy J, *et al*. The influence of lead on generation of signalling molecules and accumulation of flavonoids in pea seedlings in response to pea aphid infestation. *Molecules*. 2017;22(9):1404.
doi: 10.3390/molecules22091404
48. Kochian LV, Piñeros MA, Liu J, Magalhaes JV. Plant adaptation to acid soils: The molecular basis for crop aluminum resistance. *Annu Rev Plant Biol*. 2015;66(1):571-598.
doi: 10.1146/annurev-arplant-043014-114822